



Queensland University of Technology
Brisbane Australia

This is the author's version of a work that was submitted/accepted for publication in the following source:

[Karnowski, Karol](#), [Alonso-Caneiro, David](#), Kałużny, Bartłomiej, Kowalczyk, Andrzej, & Wojtkowski, Maciej (2012) Swept source OCT with air puff chamber for corneal dynamics measurements. In Manns, Fabrice, Söderberg, Per G., & Ho, Arthur (Eds.) *Ophthalmic Technologies XXII [Progress in Biomedical Optics and Imaging - Proceedings of SPIE]*, SPIE Press, The Moscone Center, San Francisco, CA, 82090R-1.

This file was downloaded from: <http://eprints.qut.edu.au/58068/>

© Copyright 2012 SPIE Press

Notice: *Changes introduced as a result of publishing processes such as copy-editing and formatting may not be reflected in this document. For a definitive version of this work, please refer to the published source:*

<http://dx.doi.org/10.1117/12.908848>

Swept source OCT with air puff chamber for corneal dynamics measurements

Karol Karnowski¹, David Alonso-Caneiro^{1,3}, Bartłomiej Kałużny², Andrzej Kowalczyk¹, Maciej Wojtkowski¹

¹Institute of Physics, Nicolaus Copernicus University, ul. Grudziądzka 5, PL-87 100 Toruń, Poland

²Dept of Ophthalmology, Collegium Medicum UMK, Bydgoszcz, Poland

³Contact Lens and Visual Optics Laboratory, School of Optometry, Queensland University of Technology, Brisbane, Australia

ABSTRACT

None of currently used tonometers produce estimated IOP values that are free of errors. Measurement incredibility arises from indirect measurement of corneal deformation and the fact that pressure calculations are based on population averaged parameters of anterior segment. Reliable IOP values are crucial for understanding and monitoring of number of eye pathologies e.g. glaucoma. We have combined high speed swept source OCT with air-puff chamber. System provides direct measurement of deformation of cornea and anterior surface of the lens. This paper describes in details the performance of air-puff ssOCT instrument. We present different approaches of data presentation and analysis. Changes in deformation amplitude appears to be good indicator of IOP changes. However, it seems that in order to provide accurate intraocular pressure values an additional information on corneal biomechanics is necessary. We believe that such information could be extracted from data provided by air-puff ssOCT.

Keywords: **Keywords:** Optical Coherence Tomography, Fourier domain detection methods, swept source OCT, anterior segment of the eye, cornea topographic analyses

1. INTRODUCTION

Accurate intraocular pressure (IOP) value is a crucial parameter for screening and diagnosis of glaucoma [1, 2]. Ocular hypertension is most important risk factor for glaucoma developing [3]. However, in many cases patients may suffer from so called normal-tension glaucoma. This phenomena is not completely understood and it might be caused by unusual fragility of optics nerve. Interestingly, according to Srodka[4] cornea as nonlinear structure does not fulfill Imbert-Flick law assumptions. As a result, IOP value estimated by tonometry measure is always understated when compare to real IOP. Potentially, this behavior might be somehow correlated with recently reported changes in cornea's collagenous structure as IOP is changed [5].

One of the commonly used system for IOP measurements is non-contact tonometer [2], which uses a stream of air to introduce a deformation of the cornea. The instrument monitors the dynamic behavior of the anterior surface of the cornea and estimates the value of IOP by measuring of the intensity of light reflected from the corneal surface. The intensity profile together with a profile of pressure generated in the air puff chamber can be used to calculate parameters describing corneal biomechanical properties: corneal hysteresis [1] and corneal resistance factor [6].

Recently it was presented that the cornea biomechanical properties can influence the IOP recording and thus should be taken into consideration [7-9]. Corneal thickness, the radius of curvature of the cornea and the viscoelastic properties of the eye influences the dynamics of the anterior segment during tonometry. Since anterior segment dimensions and corneal properties, based on population averages can produce an error on the estimation of IOP the clinicians usually take extra ocular measurements (i.e. pachymetry, corneal radius of curvature) to compensate for deviations [2].

None of the commonly used commercial tonometers take simultaneous recordings of dynamics of corneal and lens layers. In 2010 Oculus introduced a new noncontact tonometer using high-speed Scheimpflug camera to record corneal response to air pulse[10]. Little information about this instrument is available so far. It takes approximately 4000 frames/sec and allows dynamic inspection of both cornea surfaces during deformation.

Optical coherence tomography (OCT) techniques have proved its applicability for imaging of the posterior [11] as well

as the anterior surface of the eye [12-14]. This noninvasive optical method allows measurements with micrometer resolution and millimeter imaging depth. Fourier-domain OCT (ssOCT – swept source OCT) using wavelength tunable lasers is promising tool for 3D and functional analysis of anterior segment [15-16] since high repetition rates of swept sources are feasible. Especially sources at 1300 nm central wavelength allows better penetration into tissues such as iris, sclera or anterior chamber angle.

In this manuscript we present details on optimized ssOCT setup that was combined with an air puff chamber adapted from commercial non-contact tonometer. System allows to collect M-scans during cornea deformation induced by an air stream. The applicability of such a system to evaluate the biomechanics of cornea and its potential use to provide more accurate intraocular pressure values is presented.

2. METHOD AND RESULTS

Details on the ssOCT setup were given elsewhere [17]. For this study a commercial swept source laser working at 50 kHz with a 100 nm optical bandwidth is used (Axsun Technologies Inc., Billerica, MA). The axial resolution of the system is 9 μm in air. Modified configuration of main imaging interferometer allows to overcome power losses on air chamber double pass. For 2.5 mW optical power illuminating the eye sensitivity of 102 dB at 12 μs exposure time was measured. Spectral fringes are detected with dual balance photodiode (Thorlabs 75 MHz) and recorder (Fig1 – green line) with two channel acquisition card (Compuscope 14200, GaGe Applied Technologies, Locport, IL). Due to high laser stability, calibration fringes are recorded once per measuring session and throughout the session reference pressure in air chamber is recorded (Fig1 – blue lines).

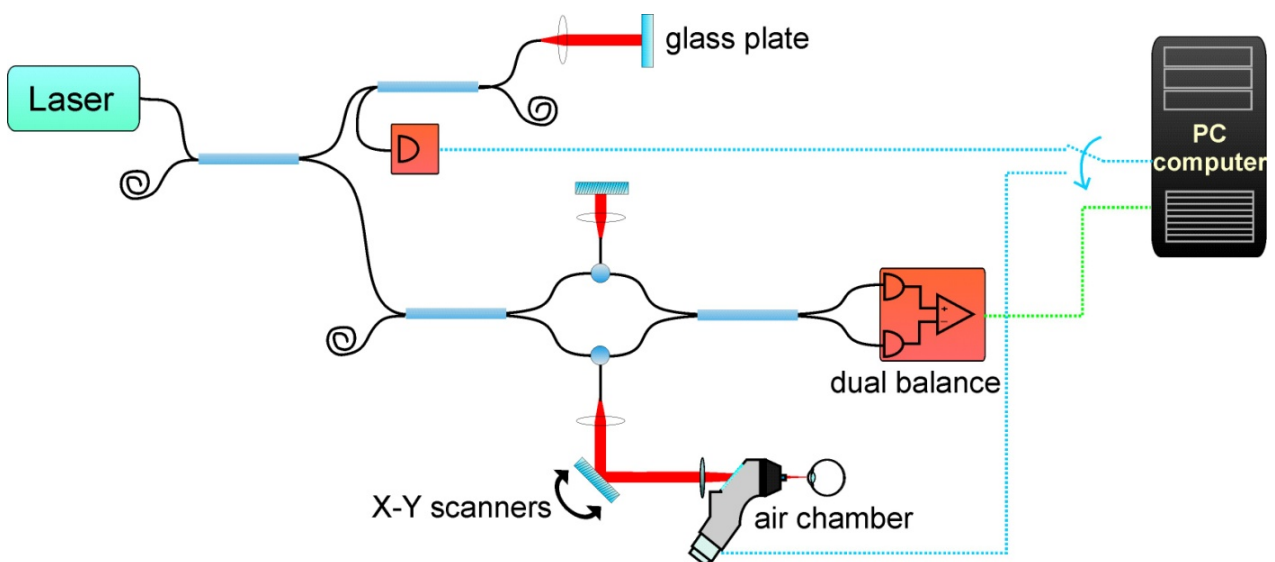


Figure 1. Diagram of air-puff ssOCT system. Upper common path interferometer generates calibration fringes using glass plate. Main interferometer optimized for power losses and balance detection.

The sample arm of the system is merged with air puff chamber (Fig2a). System of air stream generation, which is synchronized with the acquisition system and scanners. The imaging beam exits chamber through the 3mm tube. The tube delivers air puff that applanates the cornea. M-scan – a set of A-scans measured in time at the same position on cornea (Fig2c – red dot) is used as main measuring protocol. Coaxial configuration of imaging beam and air chamber ensures that measure is taken exactly in the center of applanation area. It is possible to use 2D (preview mode) and 3D scanning. Imaging through the tube is limited to 2mm in diameter and is encircled by shadow cast by the tube walls (Fig2c – blue circle). Since the tube is mounted to the chamber with disc transparent to 1300nm, it is possible to extend imaging beyond the tube. The outer imaging area is limited by the size of the mounting disc and glass window of the chamber (8mm, green circle on Fig2c). Part of 3D image that is not measured through the tube is shifted in z-axis due

longer optical distance light has to pass for tube mounting disc. Constant shift value allows for post processing corrections of that effect.

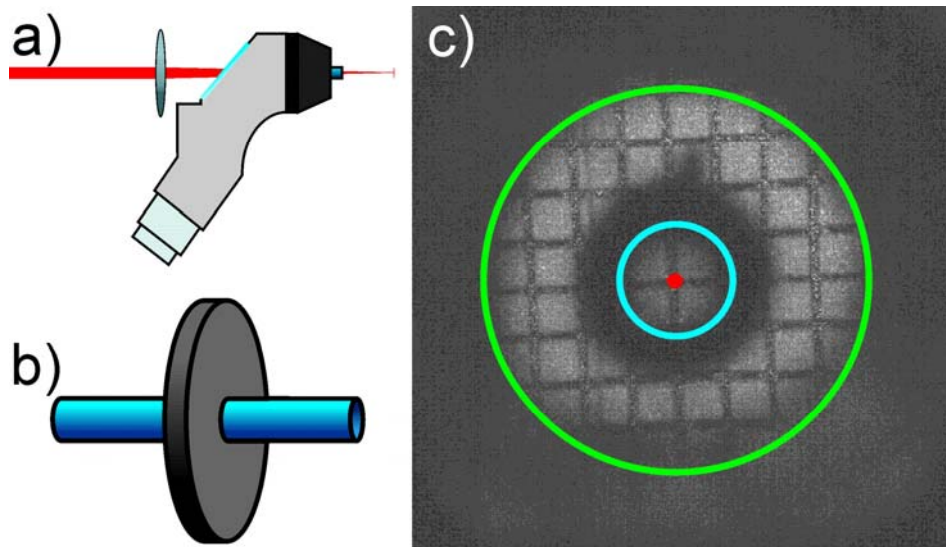


Figure 2. Limitations of imaging head. Light is delivered through the glass window (a) and exits air chamber through tube mounted on disc transparent to 130 nm (b). 3D imaging is limited to 2 mm inner area (as presented on *En face* projection of 3D data set for target with equally spaced parallel lines) and 8 mm outer area (more details in text).

During the main measuring protocol a M-scan is recorder (Fig 3). The displacement of anterior and posterior cornea surfaces and also anterior lens surface is visible. Since the M-scan is not corrected for refractive indexes the lens surface is apparently displaced towards the applanating force. The applanation and recovery process is fast enough (~15 ms) that motion artifacts can be neglected. In fact, patient reacts by closing eyelid significantly later than cornea returns to its initial position – usually 35-40ms after applanation starts.

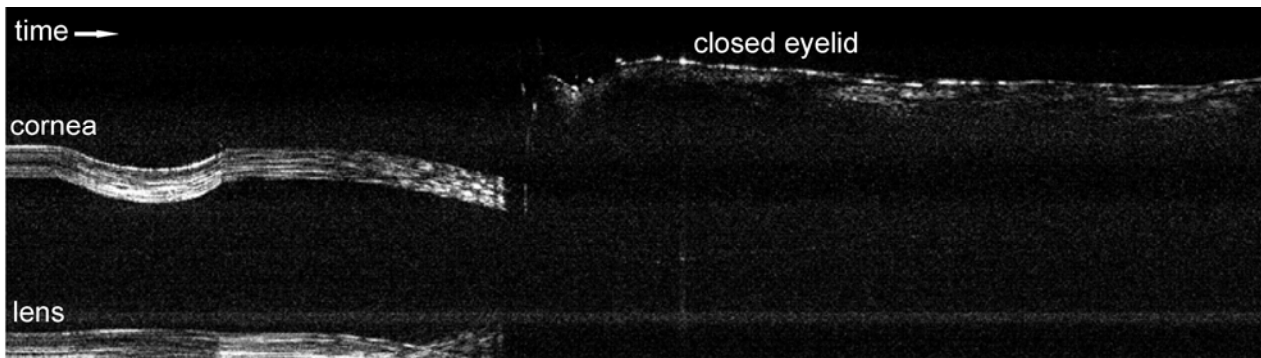


Figure 3. An example of main measure protocol – M-scan (120ms span). Only ~20 ms part - where deformation can be seen - is analyzed. In most cases after 30-35 ms reaction of patient (close eyelid) can be observed. The depth range of M-scan is ~9mm.

Segmentation procedure enables detecting positions of corneal and lens surfaces during deformation. The relative displacement of anterior corneal surface, posterior corneal surface and anterior lens surface during the applanation/recovery process is plotted (Fig 4). Plots can be used to extract quantitative parameters of deformation process: corneal anterior surface deformation amplitude (Fig4 - 1), corneal posterior surface deformation amplitude (Fig4 - 2), corneal thickness for chosen deformation point (Fig4 - 3), anterior lens surface deformation amplitude (Fig4 - 4), amplitude of chamber depth change (Fig4 - 5), deformation time (Fig4 - 6) as well as loading time and unloading

time(Fig4 – 7 and 8 respectively). Additionally deformation speed can be calculated for loading and unloading deformation periods.

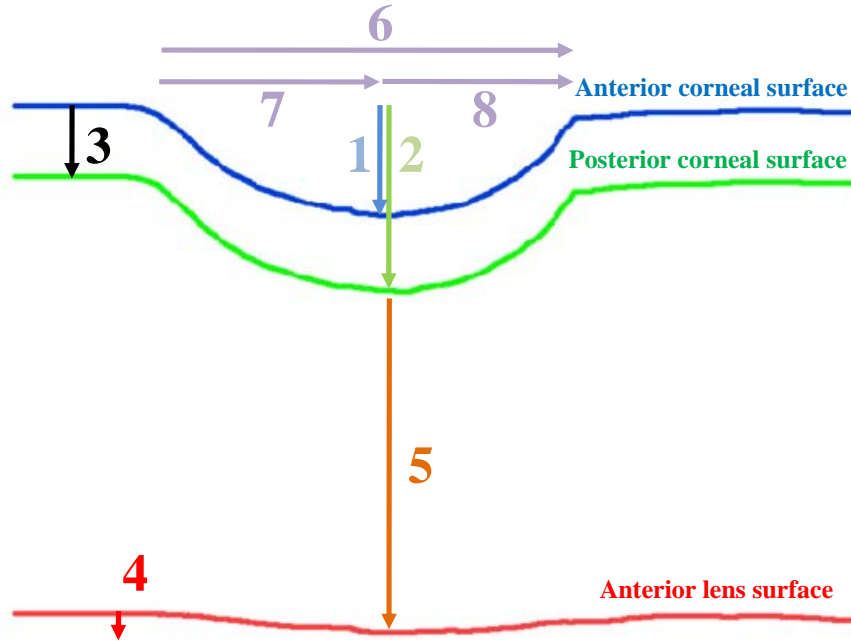


Figure 4. Deformation plots of corneal surfaces and anterior surface of the lens. Numbers indicates deformation parameters described in text.

To verify system performance a repeatability test was performed. Healthily volunteer eye was measured 10 times in 1-1.5 minute steps. For anterior cornea surfaces deformation amplitudes and amplitude of chamber depth change mean values, SD- standard deviation and percentage change were calculated (Table 1). Significant repeatability improvement was observe after short training of both patient and object. Authors believe that further improvement will be possible by adding fixation to the system.

Table 1. Repeatability performance of ssOCT based tonometry system

	Anterior cornea surface deformation amplitude	Posterior cornea surface deformation amplitude	Maximum Anterior chamber depth
Untrained operator & object			
Mean [μm]	667.2	705.5	2554
SD [μm]	41.40	58.80	78.70
%	6.2 %	8.3 %	3 %
Trained operator & object			
Mean [μm]	572.8	610.2	2173
SD [μm]	4.88	20.88	36.5
%	0.8 %	3.4 %	1.6 %

To evaluate performance of the system and understand the nature of the measurement a set of well controlled experiments was performed. Healthy eyes were measured in baseline condition. IOP was independently measured with commercial tonometer (Tono-Pen, Reichart Inc., Buffalo, NY). Drops decreasing IOP were applied for all subjects. An hour after air-puff ssOCT as well as tonometer measurements were repeated. In all cases as IOP decreased increasing in

deformation amplitudes for both corneal surfaces were observed. For example IOP change from 14 mmHg to 10.3 mmHg corresponds to change in anterior corneal surface deformation amplitude from 624 μm to 675 μm and change from 771 μm to 820 μm for posterior surface deformation amplitude.

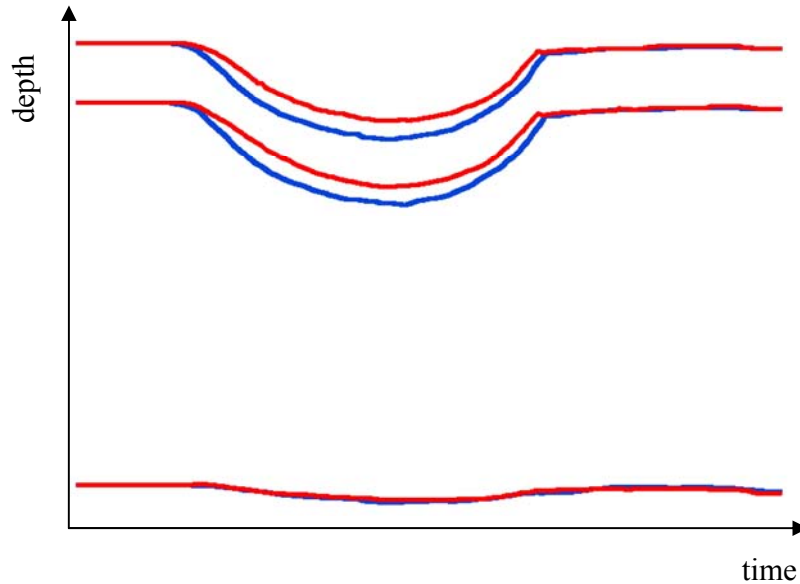


Figure 5. Change in deformation plots as an effect of applying IOP decreasing drops. Red plots corresponds to pressure of 14 mmHg, blue ones to 10.3 mmHg.

IOP changes are also noticeable when normalized deformation is plotted as a function of normalized applied pressure (Fig 6). Pressure changes as small as 1 mmHg are clearly visible (left side of Fig 6).

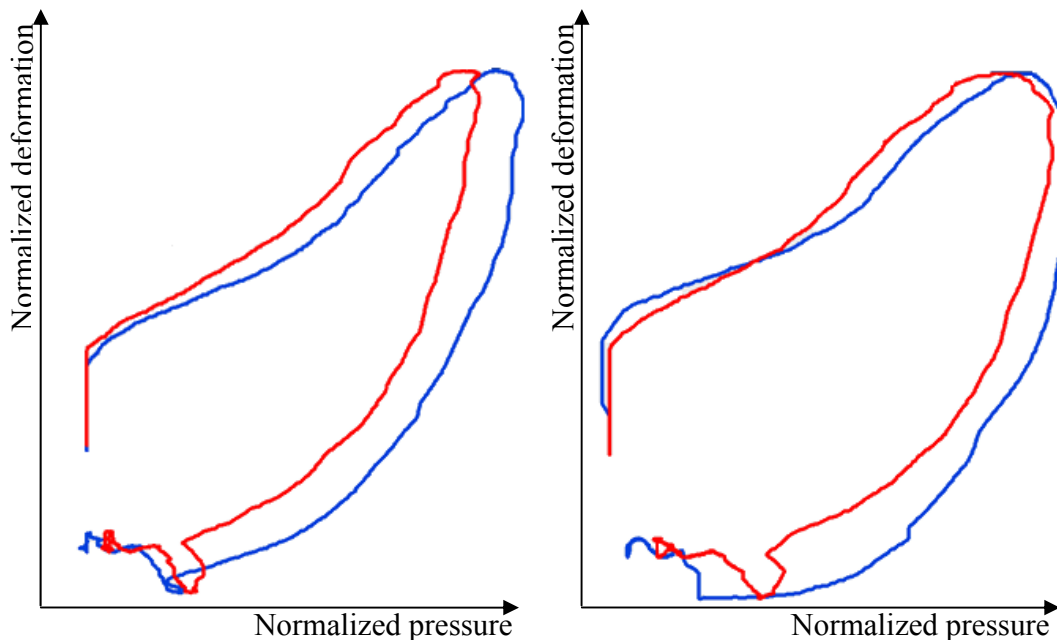


Figure 6. Normalized deformation of anterior corneal surface plotted as a function of normalized pressure in air chamber. Left side: measured for 11 mmHg IOP (red) and one hour after applying IOP decreasing drops – 10 mmHg; Right side: measured for IOP change from 12 mmHg to 8 mmHg

Although, for all subjects decrease in IOP is observed, the magnitude of those changes differs from eye to eye. Interestingly, measurements with comparable IOP changes not always provides comparable changes in deformation amplitudes. To understand this behavior further experiments have to be carefully planned and performed.

3. CONCLUSIONS

In this study the high speed ssOCT system combined with air puff chamber was presented. The instrument allows for investigation of corneal and anterior lens surface dynamics during the corneal applanation/recovery process. Sets of experiments on healthy eyes were performed to validate system performance. Analysis that were conducted show system sensitivity to IOP changes. However, changes in deformation amplitudes could possibly be also by corneal biomechanics. Thus, it might be necessary to include an analysis of corneal biomechanics to provide reliable IOP values.

4. ACKNOWLEDGEMENTS

This work was supported by EuroHORCs-European Science Foundation EURYI Award EURYI-01/2008-PL (M. Wojtkowski) and Polish Ministry of Science and Higher Education Grant N N402 084435 (B. J. Kaluzny). K. Karnowski acknowledges support from Polish Ministry of Science and Higher Education Supervisor Grant N N402 482039, Foundation for Polish Science - travel grant, the grant of the European Social Fundation and Polish Government within Integrated Regional Development Operational Programme, Action 8.2 by project "Krok w przyszłość - stypendia dla doktorantów III i IV edycja" of Kuyavian-Pomeranian Voivodeship and Grant for Young Scientists Development of Faculty of Physics, Astronomy and Applied Informatics. I. Gorczyńska acknowledges support from the National Centre for Research and Development, Grant No. LIDER/11/114/L-1/09/NCBiR/2010.

REFERENCES

1. D. A. Luce, "Determining in vivo biomechanical properties of the cornea with an ocular response analyzer," *J. Cataract Refr. Surg.* **31**, 156-162 (2005)
2. R. L. Stamper, "A history of intraocular pressure and its measurement," *Optometry Vision Sci.* **88**, E16-E28 (2011)
3. Glaucoma Overview from eMedicine
4. Sródka W, Iskander DR, "Optically inspired biomechanical model of the human eyeball," *J Biomed Opt.* 2008 Jul-Aug;13(4):044034
5. Y.-Q. Soh, S. Rehman, C. Sheppard, R.W. Beerman, "Detection of IOP-related Alterations in Cornea Architecture via Second-Harmonic-Generation Imaging," *ARVO/isi* 2011
6. D. Ortiz, D. Pinero, M. H. Shabayek, F. Arnalich-Montiel, and J. L. Alió, "Corneal biomechanical properties in normal, post-laser in situ keratomileusis, and keratoconic eyes," *J. Cataract Refr. Surg.* **33**, 1371-1375 (2007)
7. K. F. Damji, R. H. Muni, and R. M. Munger, "Influence of corneal variables on accuracy of intraocular pressure measurement," *J. Glaucoma* **12**, 69-80 (2003)
8. G. J. Orsengo, and D. C. Pye, "Determination of the true intraocular pressure and modulus of elasticity of the human cornea in vivo," *B. Math. Biol.* **61**, 551-572 (1999)
9. J. Liu, and C. J. Roberts, "Influence of corneal biomechanical properties on intraocular pressure measurement: Quantitative analysis," *J. Cataract Refr. Surg.* **31**, 146-155 (2005)
10. R. Ambrósio Jr, L. P. Nogueira, D. L. Caldas, B. M. Fontes, A. Luz, J. O. Casal, M. R. Alves, and M. W. Belin, "Evaluation of corneal shape and biomechanics before LASIK," *International Ophthalmology Clinics* **51**, 11-38 (2011).
11. M. R. Hee, J. A. Izatt, E. A. Swanson, D. Huang, J. S. Schuman, C. P. Lin, C. A. Puliafito, and J. G. Fujimoto, "Optical coherence tomography of the human retina," *Arch. Ophthalmol-chic* **113**, 325-332 (1995)

12. I. Grulkowski, M. Gora, M. Szkulmowski, I. Gorczynska, D. Szlag, S. Marcos, A. Kowalczyk, and M. Wojtkowski, "Anterior segment imaging with Spectral OCT system using a high-speed CMOS camera," *Opt. Express* **17**, 4842-4858 (2009)
13. J. A. Izatt, M. R. Hee, E. A. Swanson, C. P. Lin, D. Huang, J. S. Schuman, C. A. Puliafito, and J. G. Fujimoto, "Micrometer-scale resolution imaging of the anterior eye in vivo with optical coherence tomography," *Arch. Ophthalmol-chic* **112**, 1584-1589 (1994)
14. D. Huang, Y. Li, and S. Radhakrishnan, "Optical coherence tomography of the anterior segment of the eye," *Ophthalmol. Clin. North Am.* **17**, 1-6 (2004)
15. M. Gora, K. Karnowski, M. Szkulmowski, B. J. Kaluzny, R. Huber, A. Kowalczyk, and M. Wojtkowski, "Ultra high-speed swept source OCT imaging of the anterior segment of human eye at 200 kHz with adjustable imaging range," *Opt. Express* **17**, 14880-14894 (2009)
16. Y. Yasuno, V. D. Madjarova, S. Makita, M. Akiba, A. Morosawa, C. Chong, T. Sakai, K. P. Chan, M. Itoh, and T. Yatagai, "Three-dimensional and high-speed swept-source optical coherence tomography for in vivo investigation of human anterior eye segments," *Opt. Express* **13**, 10652-10664 (2005)
17. David Alonso-Caneiro, Karol Karnowski, Bartłomiej J. Kaluzny, Andrzej Kowalczyk, and Maciej Wojtkowski, "Assessment of corneal dynamics with high-speed swept source Optical Coherence Tomography combined with an air puff system," *Opt. Express* **19**, 14188-14199 (2011)